Check for updates

Hydrological Processes

WILEY

RESEARCH ARTICLE OPEN ACCESS

What Controls the Spatial Variation in Thermal Sensitivity in a Cascades River Basin During an Extreme Heat Year?

Savannah Milburn[1] | Michael Krochta[2] | Heejun Chang[2]

[1]School of Computing, University of Georgia, Athens, Georgia, USA | [2]School of Earth, Environment, and Society, Portland State University, Portland, Oregon, USA

Correspondence: Heejun Chang (changh@pdx.edu)

Received: 11 April 2026 | **Revised:** 15 September 2026 | **Accepted:** 4 October 2026

Keywords: climate change | random forest | spatial stream network | stream temperature | thermal sensitivity

ABSTRACT

Increasing stream temperatures resulting from climate change and consequent detrimental impacts on temperature-dependent aquatic species have signalled the need to better understand how different streams respond to changes in air temperature. This research generates a new assessment of thermal sensitivity in the Clackamas River Basin, Oregon, USA by analysing how underlying geology, climate, hydrology and land cover explain spatial variation in stream thermal sensitivity. Multiple linear regression analysis using spatially explicit landscape predictors across 72 sites identified upstream High Cascades geology, elevation, baseflow index, total upstream area and upstream shrubland area as the most significant and stable predictors determining thermal sensitivity. Spatial stream network and random forest models further validated and clarified spatial influences on stream temperature and each improved performance relative to multiple linear regression. Predictors derived at the total upstream area scale were most consistently associated with thermal sensitivity when compared to local reach contributing area or 100-m wide buffer area scales. Streams underlain by High Cascades geology, with higher baseflow and greater upstream area were substantially less sensitive to air-temperature changes ($\beta = -0.27$ to -0.61). Meanwhile, higher elevation ($\beta = -0.51$ to -0.59) and lower shrubland cover ($\beta = 0.19$ to 0.30) were associated with lower thermal sensitivity. Variation in predictors retained among models appears to reflect different indicators of shared underlying processes. Furthermore, this study confirms that these predictors are statistically robust drivers of stream thermal sensitivity via regularized regression techniques. Analysing why streams are more or less climate-resilient can inform management and restoration efforts and protect cold-water habitats.

1 | Introduction

Climate change alters freshwater ecosystems through increasing air temperatures and modifying precipitation patterns, reducing cold water inputs through decreased snowpack and intensifying summertime low flow conditions in the Western United States (Boisramé et al. 2024). Projected increases in the frequency and duration of extreme heat events have also emerged as important drivers of long-term river warming (Martinez-Villalobos et al. 2025; Sun et al. 2025). Abnormally warm stream temperatures harm riverine organisms by limiting thermally suitable habitats, escalating mortality rates and reducing reproduction in the Pacific Northwest (Bowerman et al. 2021; Krochta et al. 2025). In particular, cold-water fish such as salmon have uniquely adapted

This is an open access article under the terms of the Creative Commons Attribution License, which permits use, distribution and reproduction in any medium, provided the original work is properly cited.

© 2026 The Author(s). *Hydrological Processes* published by John Wiley & Sons Ltd.

thermal tolerances; thus, warming stream temperature significantly impacts migration and spawning timings, leading to amplified fatalities (NOAA Fisheries 2021). Exacerbating these effects, increased urbanization has led to substantial increases in stream temperatures, resulting from loss of riparian shade, runoff from impervious surfaces and wastewater inputs (Kaushal et al. 2010; Timm et al. 2020).

While maximum stream temperature is important for evaluating current habitat conditions, it does not indicate how susceptible a stream is to future climatic warming. Instead, thermal sensitivity, quantified as the slope of the relationship between air temperature and stream temperature, represents how stream temperature responds to a given change in air temperature (McGill et al. 2024). The higher the thermal sensitivity, the more susceptible the stream is to rising air temperatures. Thus, identifying where and why certain streams are more sensitive to changes in air temperature will therefore inform management and restoration efforts as climate warming persists.

It is widely accepted that stream temperature changes are strongly associated with air temperature change (Caissie 2006). Therefore, a substantial amount of literature aims to derive continuous predictions of stream temperature using time-varying air temperature data combined with other atmospheric and land cover predictors (Dugdale et al. 2017; Ficklin et al. 2023). A suite of factors across spatial and temporal scales further modify stream temperature responses to air temperature (Leach et al. 2023). Riparian shading, shortwave radiation and discharge strongly regulate daily mean and maximum stream temperatures (Siegel et al. 2023; Wondzell et al. 2018), whereas at longer time scales, empirical models indicate that air temperature and seasonality better explain stream temperature variability (Weierbach et al. 2022).

A wide selection of statistical, physically-based and machine learning (ML) model approaches have been used to investigate air-stream temperature relationships (Wehrly et al. 2009; Beaupré et al. 2020; Diaz et al. 2025; Drainas et al. 2023). These approaches primarily leverage climatic, hydrologic, landscape or other process-based information to explain stream temperature dynamics over time. However, less research is focused on quantifying how spatial characteristics within stream networks influence stream thermal sensitivity through localized hydrologic, geologic, climatic and other geographic conditions. Existing literature has found common landscape predictors affecting air-stream temperature dynamics such as elevation, groundwater influence, snowmelt timing and vegetation presence (Luce et al. 2014; McGill et al. 2024; Siegel et al. 2023). Extreme atmospheric heatwave-driven effects vary among streams depending on these site characteristics, including baseflow dynamics that mediate thermal sensitivity to atmospheric forcing (van Hamel and Brunner 2024; Sun et al. 2025). The complexity present within stream thermal responses highlights the need to understand the diverse thermal profiles that exist within a watershed via studying thermal sensitivity. With a better understanding of these dynamics, land managers, wildlife specialists, conservationists and drinking water suppliers can focus on certain local characteristics to better control stream thermal systems.

Although a large amount of existing literature has utilized a combination of ML algorithms and statistical methods to study air-stream temperature in river basins, fewer studies have investigated how hydroclimatic and landscape controls vary across spatial gradients within river networks (Siegel and Volk 2019). Addressing this question requires analytical approaches capable of capturing both complex environmental relationships and the inherent spatial structure of stream networks. Statistical methods typically make assumptions of linearity between response variables and explanatory variables, potentially overlooking nonlinear relationships and complexities often present in geospatial data. In contrast, ML algorithms can more effectively model complex nonlinear relationships but generally do not account for spatial dependence among observations (Li 2024). Spatial stream network (SSN) models help address this limitation by explicitly representing the dendritic structure of river networks and the spatial autocorrelation created by flow connectivity and flow distance (Ver Hoef et al. 2006). Because nearby stream reaches often share similar thermal characteristics independent of measured landscape variables, incorporating spatial dependence is critical for accurately identifying the environmental drivers of thermal sensitivity (Ver Hoef and Peterson 2010).

An unprecedented Pacific Northwest heat dome in 2021 (Chang et al. 2021), created a unique opportunity to evaluate stream temperature responses to an extreme heat year. Across the Clackamas River Basin, Oregon, anomalously high late June air temperatures during the 2021 heat dome were accompanied by high stream temperatures across a range of monitoring locations (Figure S2.1). To explain the spatial variation of thermal sensitivity due to localized climatic, geological and hydrological influences in this watershed during a summer which included an extreme heat wave, we compared the performance of a traditional ML algorithm, random forest (RF) regression, in relation to a multiple linear regression (MLR) model using significant landscape predictors for thermal sensitivity. Additionally, we used a SSN model accounting for inherent spatial influences present in river network structures to further explain and validate influences on thermal sensitivity identified in MLR and RF models and address model specific issues while accounting for spatial autocorrelation. This work advances previous research using a suite of spatially derived landscape predictors at four spatial scales. To investigate why specific locations in streams are more or less sensitive to changes in air temperature, we asked the following questions:

1. How can landscape and reach-scale characteristics explain spatial variation in thermal sensitivity of streams within a Cascades river basin during an anomalously warm summer?
2. How do model performances and significant predictors explaining the spatial variation of thermal sensitivity converge or diverge across three different computational models (MLR, RF, SSN)?

2 | Data and Methods

Stream temperature values were collected from 72 sites across the Clackamas River Basin in northern Oregon, USA and were combined with gridded air temperature (PRISM 2021) along with spatially derived landscape predictors from a previous

10991085, 2026, 10, Downloaded from https://onlinelibrary.wiley.com/doi/10.1002/hyp.70745 by Portland State University, Wiley Online Library on [16/10/2026]. See the Terms and Conditions (https://onlinelibrary.wiley.com/terms-and-conditions) on Wiley Online Library for rules of use; OA articles are governed by the applicable Creative Commons License

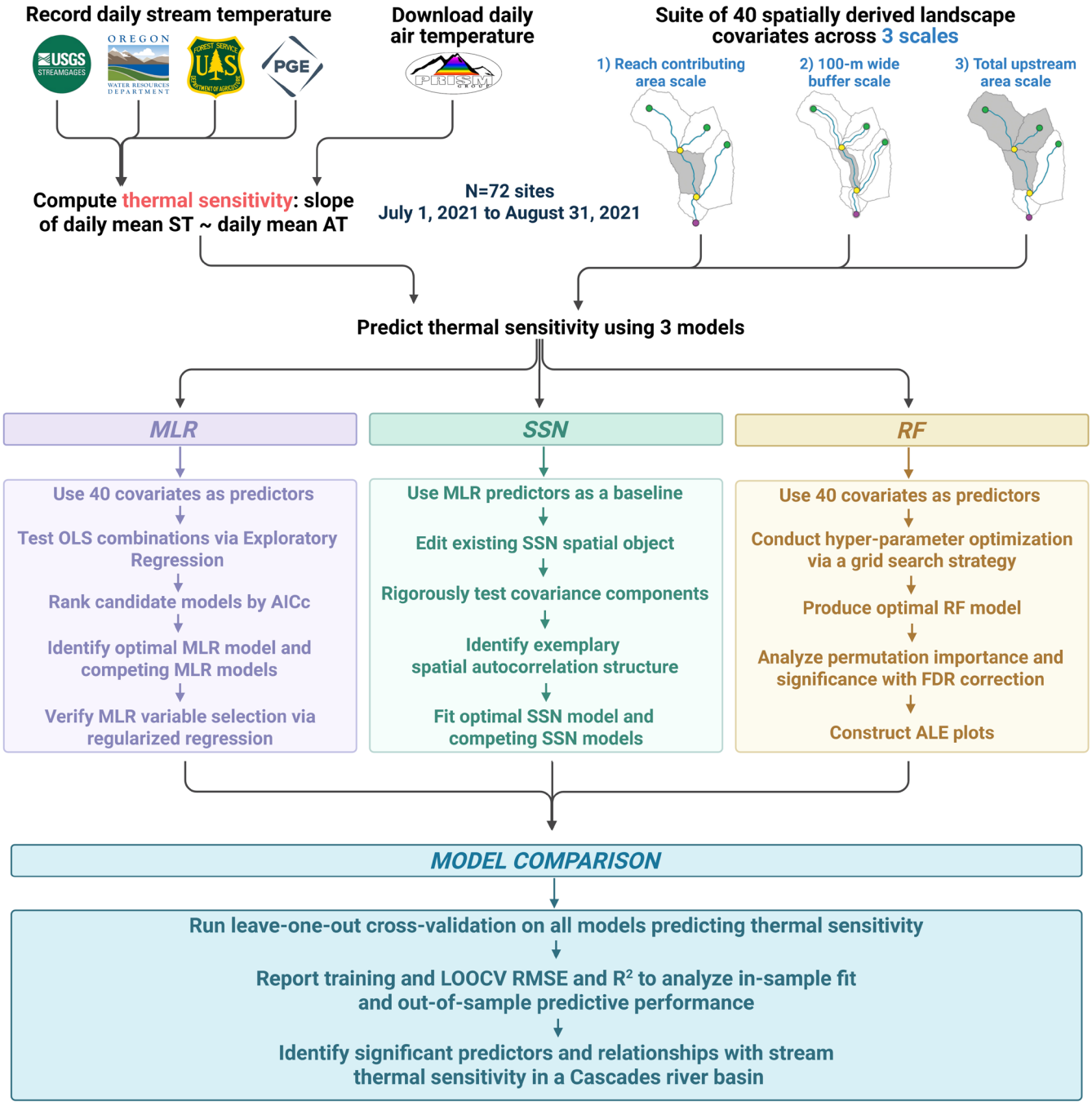


FIGURE 1 | Methodology overview of data collection process, variable selection, thermal sensitivity computation and usage of three computational models, multiple linear regression (MLR), random forest (RF) and spatial stream network (SSN), to identify significant drivers of thermal sensitivity. Predictors were derived at one of three spatial scales (Krochta and Chang 2024).

study, Krochta and Chang (2024). This data was used to build MLR models for predicting thermal sensitivity at a given site to identify the most significant landscape predictors. Regularized regression assessed predictor stability, ensuring predictors identified by models were statistically stable. SSN models were created using the same five significant predictors of thermal sensitivity from the MLR formulas to reveal any inherent spatial influences that affect thermal sensitivity. Finally, an RF model predicting thermal sensitivity was derived to further explain spatially dependent landscape and climatic influences on thermal sensitivity without assuming linearity (Figure 1).

2.1 | Study Area

The Clackamas River begins in the Cascade mountain range in northwestern Oregon and flows northwest through Mt. Hood National Forest to its confluence with the Willamette River 134 km downstream at Oregon City. The basin has a mixed

10991085, 2026, 10, Downloaded from https://onlinelibrary.wiley.com/doi/10.1002/hyp.70745 by Portland State University, Wiley Online Library on [16/10/2026]. See the Terms and Conditions (https://onlinelibrary.wiley.com/terms-and-conditions) on Wiley Online Library for rules of use; OA articles are governed by the applicable Creative Commons License

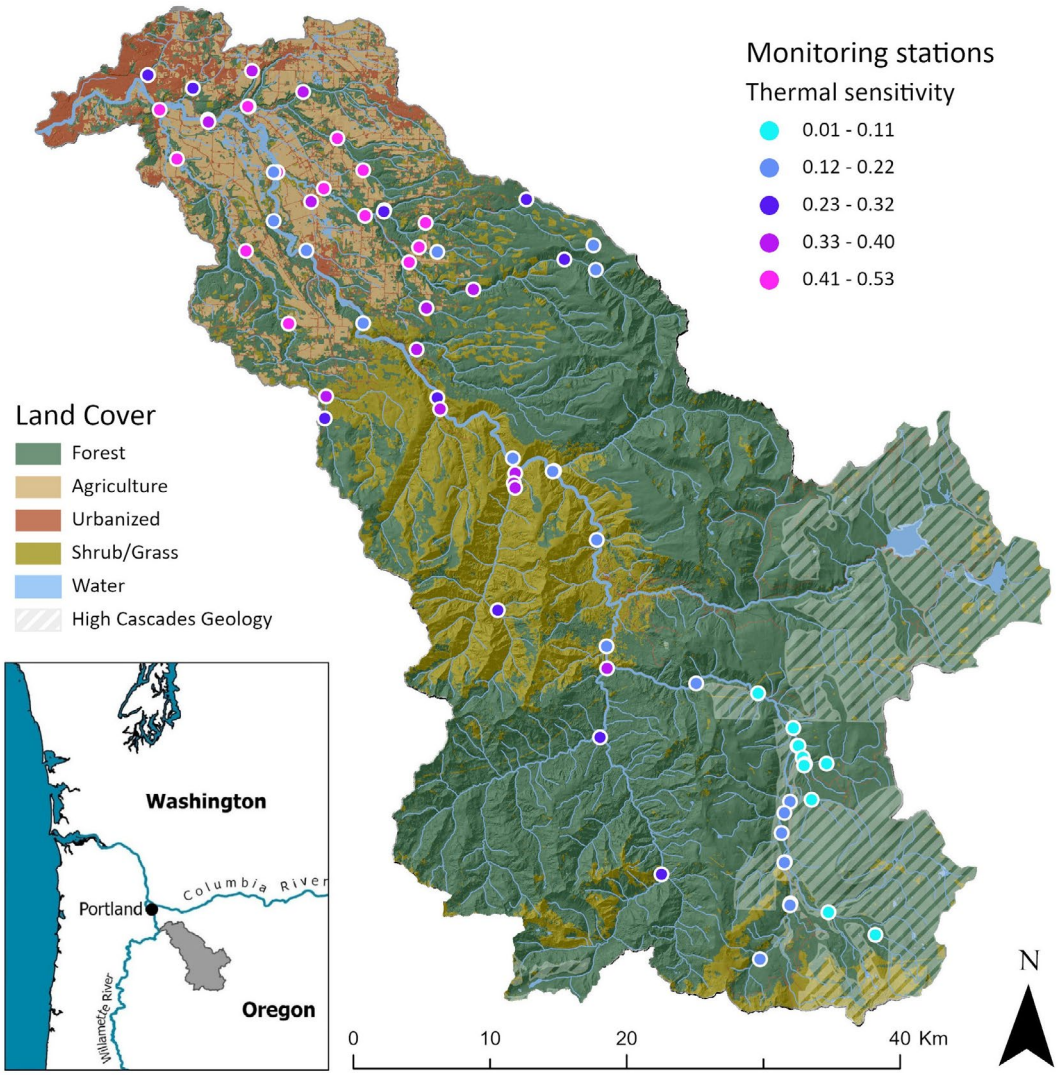


FIGURE 2 | Clackamas River Basin land cover distribution, High Cascades geology extent and sample locations with derived thermal sensitivity values. Values represent change in stream temperature (°C) with one degree increase in air temperature (°C).

geology moving from the lower basin to upper basin by following the mainstem: fluvial mudstone and sandstone, mixed grain sediments, basalt in Boring Volcanic field and Columbia River Basalt group to Cascade volcanic rocks (Oregon Department of Geology and Mineral Industries 2020). The relatively young High Cascade volcanic rocks in a high-elevation range of the basin serve as a reservoir of groundwater, replenishing streams during the dry period (together with snowmelt), while older Western Cascade and the valley areas in the middle to lower part of the basin are rainfall and surface-water dominated. This hydrologically, geologically and climatically varied river basin drains an area of 1500 km^2 to the Clackamas River, which provides high-quality drinking water for over 300 000 people within the Portland metropolitan area (State of Oregon Department of Environmental Quality 2019). Thanks to the constant groundwater input from the upper basin, the Clackamas River provides habitat for significant runs of steelhead, Coho and Chinook salmon (Native Fish Society 2022) as well as recently re-introduced bull trout (Starcevich 2021). However, portions of the basin regularly exceed Oregon's temperature standards (State of Oregon Department of Environmental Quality 2025).

The basin is composed of 16 diverse subwatersheds, each with unique landscapes and varying climates: coniferous forests take up a majority of the upper watershed along with large patches of shrub land cover in the middle basin where wildfires occurred in 2020 (USGS 2021; Figure 2). The lower parts of the watershed are largely rural agricultural along with urban developed areas closer to Portland (USGS 2021). The Clackamas River Basin has a Mediterranean climate with cool, wet winters and warm, dry summers, where air temperature, precipitation and snowpack vary strongly with elevation (Krochta et al. 2025). In contrast to these typical conditions, the June 28, 2021 Pacific Northwest heat dome drove air temperatures above 38°C for three consecutive days, peaking at 47°C in nearby Portland and producing the highest recorded mean and maximum stream temperatures on record in local streams (Supporting Information Section S2; Chang et al. 2021). Climate change is projected to further increase stream temperatures by approximately 1.4°C to 2.0°C by the mid-21st century, reducing thermally suitable habitat for cold-water salmonids by an estimated 27% to 36% (Krochta et al. 2025).

10991085, 2026, 10, Downloaded from https://onlinelibrary.wiley.com/doi/10.1002/hyp.70745 by Portland State University, Wiley Online Library on [16/10/2026]. See the Terms and Conditions (https://onlinelibrary.wiley.com/terms-and-conditions) on Wiley Online Library for rules of use; OA articles are governed by the applicable Creative Commons License

2.2 | Data Collection

2.2.1 | Air and Stream Temperature Data

We used stream temperature data from 72 sites that represented a wide range of land cover, topological, geological and climatic gradients and possessed complete records of summer stream temperature data. Daily stream temperature was recorded every 30 min and was sourced from temperature loggers from multiple local, state and federal agencies (Krochta and Anlauf-Dunn 2025). All 72 data collection sites had no gaps in stream temperature data collection between the period July 1, 2021 and August 31, 2021. Daily air temperature data for each site was downloaded for the period July 1, 2021 to August 31, 2021 at 4 km resolution from the Parameter-elevation Regressions on Independent Slopes Model (PRISM) Group at Oregon State University (PRISM 2021). Although widely used, this 4-km spatial resolution may not capture fine-scale air temperature variability in complex terrain.

2.2.2 | Spatial Landscape Predictor Data

Spatial topological, hydrological and climatic predictors were derived from a suite of 40 different landscape variables across four different spatial scales: total upstream area-scale landscape predictors, stream reach contributing area-scale (RCA) landscape predictors, 100-m wide buffer-scale landscape predictors and stream reach-specific predictors (Table 1; Krochta and Chang 2024). Climatic variables were only summarized at the catchment scale because the spatial resolution of the datasets made the RCA the smallest meaningful unit of analysis. Stream channel slope and baseflow index (BFI) were obtained as pre-calculated NHDPlus Version 3 (USGS 2012) reach attributes and are only available at the reach-specific scale, with elevation also defined as the elevation of the specific stream reach.

2.3 | Methods

2.3.1 | Air-Stream Temperature Relationship and Thermal Sensitivity Calculation

Thermal sensitivity values for each of the 72 sites in the Clackamas River Basin were calculated using two summary metrics: daily mean air temperature and daily mean stream temperature. Daily mean stream temperature for each site was computed by finding the average stream temperature value from July 1, 2021 to August 31, 2021 using R version 4.4.2 (R Core Team 2024). Daily mean air temperature for each site was downloaded using each site's coordinates to extract daily mean air temperature rasters from PRISM (PRISM 2021) over the same period. The thermal sensitivity value for each site was then computed by using a bivariate linear regression model of each site's daily mean stream temperature and daily mean air temperature across the July 1 to August 31, 2021 date range. The slope of each site's linear regression model represents the change in daily mean stream temperature for every 1°C increase in daily mean air temperature from July 1 to August 31, 2021.

2.3.2 | Variable Selection Procedure and Multiple Linear Regression Model for Predicting Thermal Sensitivity

Multiple linear regression (MLR; Equation 1) was used as a baseline model of the relationship between stream thermal sensitivity and the various environmental predictor variables:

$$y = X\beta + \varepsilon \quad (1)$$

where y is the vector of observed stream thermal sensitivity values, X is the matrix of predictors (Table 1), β is the vector of regression coefficients and ε is a vector of independent residual errors.

MLR variable selection was conducted using the Exploratory Regression tool in ArcGIS Pro version 3.0.0 (ESRI 2022) to identify parsimonious combinations of predictors associated with stream thermal sensitivity from the initial pool of 40 candidate variables. The tool systematically evaluates combinations of candidate explanatory variables using ordinary least squares regression and assesses candidate models based on model fit and diagnostic criteria, including adjusted R^2, coefficient significance, multicollinearity (variance inflation factor; VIF), residual normality (Jarque–Bera test) and spatial autocorrelation of model residuals (Global Moran's I) (ESRI 2026). Default diagnostic thresholds were used, requiring an adjusted $R^2 \geq 0.50$, coefficient p-values < 0.05, VIF ≤ 7.5, Jarque–Bera $p > 0.10$ and residual spatial-autocorrelation $p > 0.10$. Candidate models were ranked using Akaike Information Criterion corrected for small sample sizes (AICc), with lower values indicating greater relative support. The model with the lowest AICc was identified as the top-supported model and models within two AIC units of the top model (ΔAICc ≤ 2) were retained as similarly supported candidate models (Burnham and Anderson 2002). The predictors contained in the top-supported models were subsequently used in the final MLR analysis.

To evaluate whether this variable selection procedure was robust to sampling variability and consistently identified thermal sensitivity relationships across the basin, three regularized regression techniques—ridge, LASSO and elastic net—were each implemented using a geographic 5-fold cross-validation (Roberts et al. 2017; Tibshirani 1996; Zou and Hastie 2005). Sites were ordered from north to south and divided among five folds to ensure that observations were systematically distributed across the geographically diverse Clackamas River Basin. For each regularization technique, models were fit across the five folds, allowing the stability of predictors to be evaluated across different subsets of the data. Ridge regression provided an assessment of coefficient stability under continuous shrinkage, while LASSO and elastic net additionally allowed further evaluation of variable selection consistency. This approach provided an independent assessment of whether predictors identified by the MLR variable selection procedure remained supported under regularization and across folds, addressing potential selection bias associated with data-driven stepwise procedures (Tredennick et al. 2021). Full methodological details and stability results are reported in Supporting Information Section S1.

10991085, 2026, 10, Downloaded from https://onlinelibrary.wiley.com/doi/10.1002/hyp.70745 by Portland State University, Wiley Online Library on [16/10/2026]. See the Terms and Conditions (https://onlinelibrary.wiley.com/terms-and-conditions) on Wiley Online Library for rules of use; OA articles are governed by the applicable Creative Commons License

TABLE 1 | Suite of 40 landscape predictors separated by category and labelled with their data source and hypothesized relationship with stream thermal sensitivity.

Category	Landscape predictor/ hypothesized relationship	Data source	Spatial scale			
			Stream reach-specific	100-m buffer	Reach contributing area	Total upstream area
Geomorphology	Base flow index (–)	USGS (2012)	X			
	High Cascades geology % (–)	Oregon Department of Geology and Mineral Industries (2020)		X	X	X
	Stream channel slope (–)	USGS (2012)	X			
Topology	Elevation (m) (–)	Oregon Department of Geology and Mineral Industries (2020)	X			
	Solar exposure (+)	Oregon Department of Geology and Mineral Industries (2020)			X	
	Upstream area km (–)	USGS (2012)				X
Land Use	Agricultural land area % (+)	USGS (2021)		X	X	X
	Developed land area % (+)	USGS (2021)		X	X	X
	Road density (+)	Clackamas County (2022)		X	X	X
Vegetation	Forest area % (–)	USGS (2021)				X
	Shrubland area % (+)	USGS (2021)				X
	Vegetation cover (–)	Landfire (2022)		X	X	X
	Vegetation height (–)	Landfire (2022)		X	X	X
Wildfire	Burned land area % (+)	USGS et al. (2022)		X	X	X
Water area	Lakes area % (+)	USGS (2021)		X	X	X
	Wetlands area % (+)	USGS (2021)		X	X	X
Climate	Annual ppt (mm) (–)	PRISM (2021)			X	
	Summer ppt (mm) (–)	PRISM (2021)			X	
	Wet season ppt (mm) (–)	PRISM (2021)			X	
	Summer max AT (°C) (+)	PRISM (2021)			X	
	Summer mean AT (°C) (+)	PRISM (2021)			X	
	Summer mean max AT (°C) (+)	PRISM (2021)			X	

Note: All variables were sourced from Krochta and Chang (2024).

2.3.3 | Spatial Stream Network Model for Predicting Thermal Sensitivity

Spatial stream network (SSN; Equation 2) models (Peterson and Ver Hoef 2010) were constructed to simulate thermal sensitivity across the basin and compare model performance with statistical (MLR) and machine learning (RF) models. SSN models extend linear regression by incorporating spatially correlated random effects that account for autocorrelation within dendritic stream networks:

$$y = X\beta + z_{TU} + z_{TD} + z_E + \varepsilon \quad (2)$$

where y is the vector of observed stream thermal sensitivity values, X is the matrix of predictor variables, β is the vector of regression coefficients, z_{TU}, z_{TD} and z_E are spatial random

10991085, 2026, 10, Downloaded from https://onlinelibrary.wiley.com/doi/10.1002/hyp.70745 by Portland State University, Wiley Online Library on [16/10/2026]. See the Terms and Conditions (https://onlinelibrary.wiley.com/terms-and-conditions) on Wiley Online Library for rules of use; OA articles are governed by the applicable Creative Commons License

effects associated with the tail-up, tail-down and Euclidean covariance structures, respectively, and ε is a vector of independent residual errors.

The SSN object from a previous Clackamas River study (Krochta et al. 2025) was edited by including only the predictors specified by the best-performing MLR formulas based on AICc (Figure 1), adding the response variable, thermal sensitivity, to the SSN spatial object, originally created using the SSN R package (Ver Hoef et al. 2014). Rigorous pre-processing occurred to ensure that the SSN spatial object possessed no duplicates and unique sites following editing the SSN object. After computing new distance matrices for the updated SSN object, testing occurred to determine every possible combination of spatial components across the three arguments available in the SSN2 package (tail-up, tail-down and Euclidean) (Dumelle et al. 2024) under R version 4.4.2 (R Core Team 2024). Based on all possible combinations, best-performing SSN models were selected based on AIC, the amount of variability explained by each covariance component (de parameter), amount of autocorrelation (range parameter) and overall variance explained. This top-performing structure of spatial covariance components was applied identically across all SSN models to isolate the effect of variable selection from spatial covariance structure.

2.3.4 | Random Forest Model for PREDICITING Thermal Sensitivity

The same suite of 40 landscape predictors (Table 1) was used to create a random forest regression (RF; Equation 3) model predicting thermal sensitivity without assuming linearity (Breiman 2001). RF predicts the response as the average prediction across an ensemble of regression trees:

$$\hat{y}(x) = \frac{1}{B}\sum_{b=1}^{B} T_{b(x)} \tag{3}$$

where $\hat{y}(x)$ is the predicted response for observation x, B is the number of regression trees and $T_{(b)(x)}$ is the prediction from the b^{th} regression tree. Each tree is built using a bootstrap sample of the data while considering a random subset of predictors at each split.

The h2o package (Fryda et al. 2024) under R version 4.4.2 (R Core Team 2024) was used to execute a grid search strategy in order to find the optimal hyperparameters for a best RF model derived by considering all 40 landscape predictors. The specific parameters selected during hyper parameter optimization included 400 decision trees, a max depth of 25 and a sample rate of 0.7. After finding this best RF model, permutation importance scores were computed for the top six most important features in the best RF model, independent of the predictors selected by the MLR analysis, in order to identify controlling drivers of thermal sensitivity found by the RF model without assuming linearity using the ranger package (Wright and Ziegler 2017) under R version 4.4.2 (R Core Team 2024).

Permutation-based significance testing for importance scores was computed using the importance_pvalues() function in the ranger package (Wright and Ziegler 2017) to test whether each RF-selected predictor's permutation importance exceeds what would be expected by chance (Altmann et al. 2010). The thermal sensitivity response variable was permuted 1999 times with the RF model refit each time using the fixed optimal hyperparameters noted above, building an empirical null distribution for each predictor. This test was run on the full 40-predictor model with Benjamini–Hochberg false discovery rate (FDR) correction applied across all predictors (Benjamini and Hochberg 1995). Raw permutation importance scores were normalized to each predictor's proportional share of total importance across all 40 predictors (summing to one) for interpretability.

To visualize nonlinear relationships between significant predictors identified by the RF model and thermal sensitivity, Accumulated Local Effects (ALE) plots were constructed (Apley and Zhu 2020) using the iml package (Molnar et al. 2018) under R version 4.4.2 (R Core Team 2024). Given the substantial correlation structure and zero-inflated distributions documented in our suite of 40 predictors, ALE plots were used instead of partial dependence plots (PDPs) because ALE computes local, quantile-based neighbourhoods of observed data instead of substituting swept values into every observation regardless of whether that combination occurs in the data, avoiding extrapolating into predictor combinations with minimal real data support (Hooker et al. 2021). ALE plots do not include significance testing of local effects because no established method exists for this purpose; thus, global significance of each predictor is assessed via the permutation-based significance test described above.

2.4 | Model Comparison Using Cross-Validation

To enable direct comparison across model classes, a leave-one-out cross-validation (LOOCV) was performed on the MLR, SSN and RF models. LOOCV was used as the primary cross-validation scheme due to the SSN model's inherent spatial autocorrelation and protection against significant impacts to the SSN spatial object's structure when leaving out a fold of multiple sites (Ver Hoef et al. 2014). LOOCV root mean square error (RMSE) and R^2 values were reported alongside training RMSE and R^2 values to determine how well each model could generalize to unmonitored sites, based on each model's specific structure or predictors specified.

3 | Results

Thermal sensitivity varied widely across the Clackamas River Basin with drivers of thermal sensitivity differing between the MLR and RF models. Additionally, the SSN model revealed that flow-connected spatial influences impact thermal sensitivity.

3.1 | Variation in Thermal Sensitivity

Thermal sensitivity was a dynamic value that varied significantly from site to site (Figure 2). The minimum thermal sensitivity was < 0.01 while the maximum thermal sensitivity was 0.53. Similarly, daily mean air temperature values and daily

10991085, 2026, 10, Downloaded from https://onlinelibrary.wiley.com/doi/10.1002/hyp.70745 by Portland State University, Wiley Online Library on [16/10/2026]. See the Terms and Conditions (https://onlinelibrary.wiley.com/terms-and-conditions) on Wiley Online Library for rules of use; OA articles are governed by the applicable Creative Commons License

mean stream temperature values in particular, showed substantial variation across the river basin. Daily mean air temperature ranged from 16.89°C to 21.57°C. The minimum and maximum values reported for daily mean stream temperature were 4.83°C and 21.66°C, respectively.

3.2 | Multiple Linear Regression Analysis

Exploratory regression identified three competitive models within 2 AICc units of the top-supported model (ΔAICc ≤2), with similar explanatory power across models (adjusted R^2 = 0.76 to 0.77; Table 2). The top-ranked model (Model 1) included stream elevation, upstream High Cascades geology, total upstream area, upstream shrubland area and burned buffer area (Table 2). Elevation exhibited the strongest association with thermal sensitivity (standardized $\beta = -0.59$), followed by upstream High Cascades geology ($\beta = -0.36$) and total upstream area ($\beta = -0.31$), while upstream shrubland area was positively associated with thermal sensitivity ($\beta = 0.30$) (Table 2). Burned buffer area was negatively associated with thermal sensitivity ($\beta = -0.25$) (Table 2).

The second- and third-ranked models (Models 2 and 3) received similarly strong support (Table 2). Stream elevation, upstream High Cascades geology and BFI each occurred in two of the three models, with elevation and BFI exhibiting some of the largest standardized effects across the candidate set. Across all three models, total upstream area and upstream shrubland area were consistently retained, with total upstream area negatively associated and shrubland area positively associated with thermal sensitivity. All predictors retained in the three models were statistically significant ($p < 0.01$; Table 2). Overall, the recurrence and consistent direction of several predictors across similarly supported models indicated a relatively stable set of predictors associated with spatial variation in stream thermal sensitivity.

Regularized regression supported several predictors identified by exploratory regression. Across the five geographic folds, base flow index, stream channel slope, elevation, upstream High Cascades geology, upstream shrubland area and upstream drainage area were retained in all folds by both LASSO and elastic net (Table S1.2). Full regularization results are provided in Supporting Information Section S1.

TABLE 2 | Top-supported exploratory regression models predicting stream thermal sensitivity.

Predictor/model statistic	Model 1	Model 2	Model 3
Predictor			
Elevation	−0.59	−0.51	—
Base flow index (BFI)	—	−0.51	−0.61
High Cascades geology % (upstream)	−0.36	—	−0.29
Total upstream area	−0.31	−0.41	−0.27
Shrubland area % (upstream)	0.3	0.19	0.22
Burned land area % (buffer)	−0.25	—	—
Developed land area %(upstream)	—	−0.22	—
Stream channel slope	—	—	−0.22
Model statistic			
Adjusted R^2	0.77	0.77	0.76
AICc	−170.6	−170.1	−169.2

Note: Predictor values are standardized regression coefficients (β); dashes indicate predictors not included in a model. Models shown were within two AICc units of the top-supported model (ΔAICc ≤2). Adjusted R^2 and corrected Akaike Information Criterion (AICc) are reported for each model.

3.3 | Spatial Stream Network Model Analysis

The SSN models utilized the same significant predictors derived from the MLR models. However, the three SSN models revealed that a combination of these predictor variables with flow distance and direction best explained thermal sensitivity. The specific variance components included in the SSN model were a linear tail-up component and a jbessel Euclidean component (Dumelle et al. 2024; Ver Hoef et al. 2006). Depending on the model, the variability explained by the same five predictors from the MLR formulas without accounting for spatial influences inherent in stream network structures ranged from 58.9% to 64.1%. Flow-connected spatial influences explained 34.4% to 39.5% additional variability in thermal sensitivity (tail-up variance = 20.8% to 25.2%, Euclidean variance = 13.6 to 15.5%). The local nugget influence present in stream networks explained 1.6 to 1.7% of variability in thermal sensitivity (Isaak et al. 2014; Table 3).

Across the three SSN models, upstream shrubland area was consistently positively associated with stream thermal sensitivity, while stream elevation, BFI and upstream High Cascades geology were consistently negatively associated with thermal sensitivity in models where they were included (Table 3). Upstream developed area and channel slope were also significant negative predictors in Models 2 and 3, respectively. Total upstream area is only significant in Model 2 and burned buffer land was not significant after spatial autocorrelation was accounted for.

3.4 | Random Forest Model Analysis

The most important features selected by the RF model in explaining thermal sensitivity, using permutation importance scores, differed somewhat from those identified with MLR and included: BFI, upstream High Cascades geology, upstream vegetation height, stream elevation, upstream developed land area and upstream agricultural land (Table 4). Only upstream High Cascades geology, stream elevation, BFI and upstream developed land area were common to both the RF model's independently

10991085, 2026, 10, Downloaded from https://onlinelibrary.wiley.com/doi/10.1002/hyp.70745 by Portland State University, Wiley Online Library on [16/10/2026]. See the Terms and Conditions (https://onlinelibrary.wiley.com/terms-and-conditions) on Wiley Online Library for rules of use; OA articles are governed by the applicable Creative Commons License

TABLE 3 | Standardized regression coefficients (β) for predictors of thermal sensitivity for the top-performing (1) and two competing (2 and 3) SSN models along with variance explained in thermal sensitivity by SSN model spatial components: Linear tail-up component, jbessel Euclidean component and nugget influence component.

	Model 1	Model 2	Model 3
Predictors' standardized regression coefficients (β)			
Elevation	−0.59***	−0.48***	
Base flow index (BFI)		−0.55***	−0.63***
High Cascades geology % (upstream)	−0.28**		−0.24*
Total upstream area	−0.20	−0.31***	−0.19
Shrubland area % (upstream)	0.22*	0.19*	0.24**
Burned land area % (buffer)	−0.13		
Developed land area % (upstream)		−0.21**	
Stream channel slope			−0.18**
Model statistic			
AIC	−141.2	−140.6	−149.7
Variance			
Non-spatial fixed effects	59.6%	64.1%	58.9%
Tail-up	23.2%	20.8%	25.2%
Euclidean	15.5%	13.6%	14.3%
Nugget	1.7%	1.6%	1.7%

*$p < 0.05$.
**$p < 0.01$.
***$p < 0.001$.

ranked most important predictors and the predictors selected by the MLR models.

Permutation-based significance testing across all 40 candidate predictors found all six of the most important RF predictors significant after Benjamini–Hochberg FDR correction: BFI ($p = 0.005$), upstream High Cascades geology ($p = 0.005$), upstream vegetation height ($p = 0.005$), stream elevation ($p = 0.007$), upstream developed land area ($p = 0.005$) and upstream agricultural land area ($p = 0.007$) (Table 4).

ALE plots revealed distinct nonlinear relationships between stream thermal sensitivity and the significant predictors identified by the RF model (Figure 3). BFI showed a stable effect from approximately 49% to 65% BFI but declined sharply to a negative effect above 68% BFI (Figure 3a). Thermal sensitivity declined at certain thresholds for upstream High Cascades geology and upstream vegetation height, transitioning from positive to negative effect near 20% coverage and 20 m respectively (Figure 3b,c). Elevation showed a stable positive plateau below ~300 m to a negative plateau above 700 m, supported by 14 out of 72 sites in the 700 to 850 m range (Figure 3d). The apparent continued decline beyond ~900 m is based on only three sites. The percentage of upstream developed and agricultural land area each showed a sharp increase from low or negative effects on thermal sensitivity near 0% coverage to a stable positive plateau with little variation through observed coverage ranges by 5% and 11% coverage, respectively (Figure 3e,f). The tails of both predictors are supported by relatively few sites (beyond 19% developed land coverage, $n = 4$ and beyond 30% agricultural land coverage, $n = 7$; Figure 3e,f). These threshold and non-monotonic patterns, particularly BFI's shift from positive to negative effects on stream thermal sensitivity, were not captured by the aspatial, nonlinear MLR models.

3.5 | Model Comparison

When predictive performance across the three model types was compared, the nonspatial, linear MLR models had the weakest held-out performance (LOOCV RMSE = 0.072 to 0.077, LOOCV $R^2 = 0.71$ to 0.75) with a slight decline from their

TABLE 4 | Normalized permutation importance scores of the six most important predictors of thermal sensitivity in the random forest (RF) model with permutation-based significance under BH-FDR correction applied across all 40 candidate predictors.

Importance rank	Predictors	Permutation importance	Raw *p*	BH-FDR *p*	Significant ($\alpha = 0.05$)
1	Base flow index (BFI)	0.225	0.001[a]	0.005	Yes
2	High Cascades geology % (upstream)	0.167	0.001[a]	0.005	Yes
3	Vegetation height (upstream)	0.111	0.001[a]	0.005	Yes
4	Elevation	0.092	0.001	0.007	Yes
5	Developed land area % (upstream)	0.072	0.001[a]	0.005	Yes
6	Agricultural land area % (upstream)	0.055	0.001	0.007	Yes

[a]Values at the resolution floor of 1999 permutations (minimum possible *p*-value is 1/2000 = 0.001).

10991085, 2026, 10, Downloaded from https://onlinelibrary.wiley.com/doi/10.1002/hyp.70745 by Portland State University, Wiley Online Library on [16/10/2026]. See the Terms and Conditions (https://onlinelibrary.wiley.com/terms-and-conditions) on Wiley Online Library for rules of use; OA articles are governed by the applicable Creative Commons License

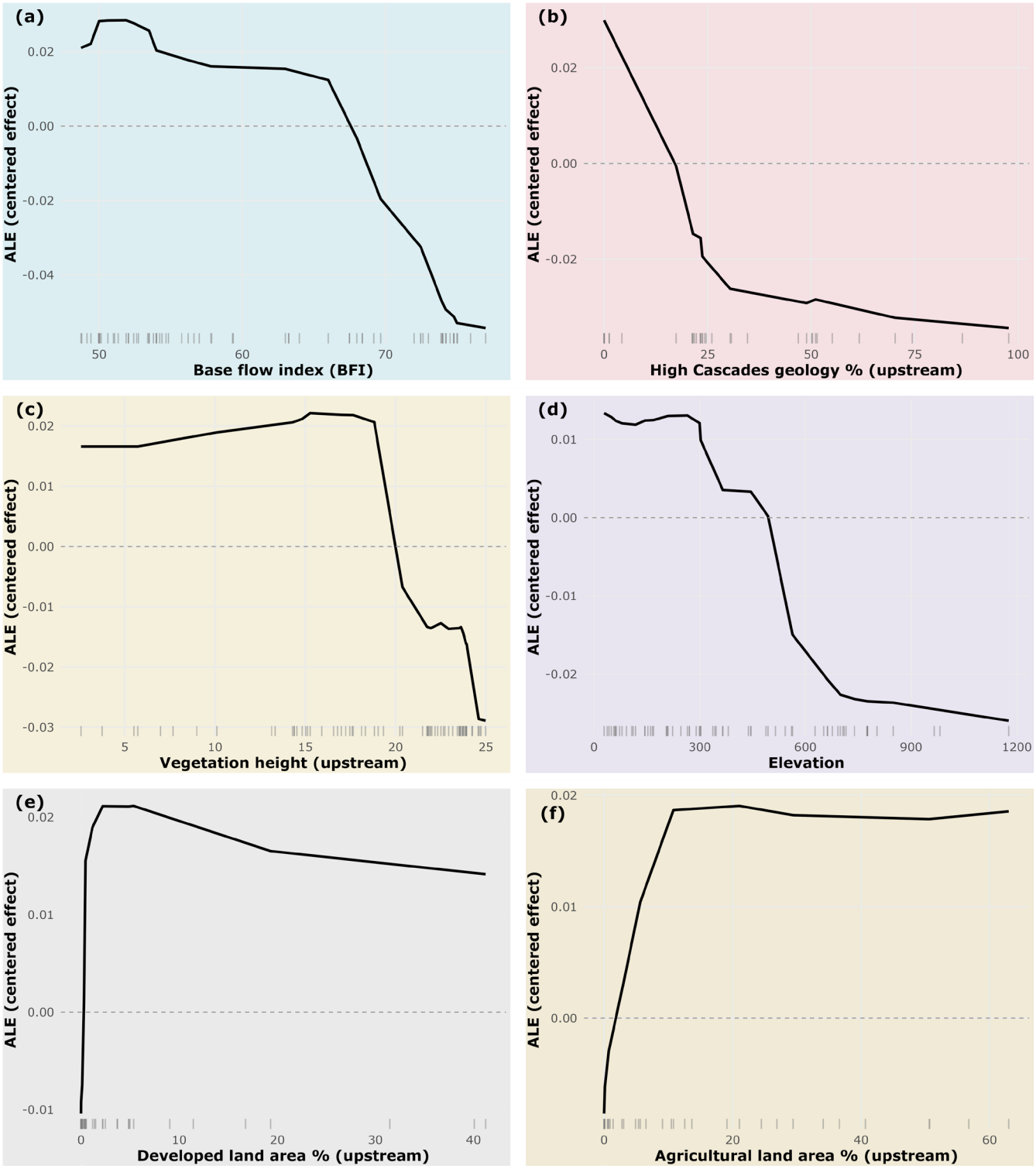


FIGURE 3 | Accumulated Local Effects (ALE) plots for the six predictors identified as significant predictors of stream thermal sensitivity by the RF model: (a) BFI, (b) High Cascades geology % (upstream), (c) vegetation height (upstream), (d) elevation, (e) developed land area % (upstream), (f) agricultural land area % (upstream). Rug marks signify observed predictor values ($n = 72$).

training performance (training RMSE = 0.066 to 0.067, $R^2 = 0.78$) (Table 5). The spatial SSN model achieved the highest held-out performance (LOOCV RMSE = 0.068 to 0.070, LOOCV $R^2 = 0.81$ to 0.85; Table 5). The nonspatial, nonlinear RF model achieved moderate held-out performance compared to MLR and SSN (LOOCV RMSE = 0.069, LOOCV $R^2 = 0.76$), which was nearly identical to its out-of-bag training estimate (RMSE = 0.069, $R^2 = 0.77$) (Table 5).

10991085, 2026, 10, Downloaded from https://onlinelibrary.wiley.com/doi/10.1002/hyp.70745 by Portland State University, Wiley Online Library on [16/10/2026]. See the Terms and Conditions (https://onlinelibrary.wiley.com/terms-and-conditions) on Wiley Online Library for rules of use; OA articles are governed by the applicable Creative Commons License

TABLE 5 | Leave-one-out cross-validation RMSEs and R^2 values along with training RMSE and RMSEs and R^2 values and number of predictors used in each computational model predicting thermal sensitivity: Multiple linear regression (MLR) models, spatial stream network (SSN) models and random forest (RF) model.

	Spatial component	# Predictors	Model	Training RMSE	Training R^2	LOOCV RMSE	LOOCV R^2
MLR	No	5	1	0.0663	0.78	0.0718	0.75
			2	0.0666	0.78	0.0717	0.75
			3	0.0670	0.78	0.0771	0.71
SSN	Yes	5	1	0.0702	0.76	0.0583	0.83
			2	0.0679	0.77	0.0547	0.85
			3	0.0685	0.77	0.0622	0.81
RF	No	40	N/A	0.0690[a]	0.77[a]	0.0694	0.760

[a]RF training metrics represent out-of-bag (OOB) performance rather than in-sample fit.

4 | Discussion

4.1 | Landscape Controls of Stream Thermal Sensitivity

Although the MLR, SSN and RF models identified somewhat different combinations of predictors, the selected variables consistently represented a common set of mechanistically distinct controls on stream thermal sensitivity, particularly hydrogeology and land cover. Closely related predictors varied among the top MLR and SSN models, suggesting that different variables may serve as proxies for shared underlying processes, while the RF model independently emphasized many of these same controls. This convergence across modelling approaches provides stronger evidence for the processes governing thermal sensitivity than any individual predictor or model alone.

Similar to previous studies of maximum stream temperature controls within the basin (Krochta and Chang 2024), landscape predictors derived at the total upstream area spatial scale were strongly associated with thermal sensitivity (Tables 2 and 4). Upstream High Cascades geology emerged as a particularly strong predictor: streams underlain by these highly porous volcanic rocks and with higher BFI were substantially less sensitive to air temperature changes (Tables 2–4). This likely reflects the greater permeability of High Cascades geology and associated cold groundwater inputs (Krochta and Chang 2024; Tague et al. 2007). Although the residence time of this groundwater and its contribution to streamflow remain uncertain, projected shifts from snowfall to rainfall are expected to alter groundwater recharge processes, with potential implications for the magnitude and timing of cold groundwater inputs to streams (Nolin 2012; Tague et al. 2008). Moreover, High Cascades geology, BFI and total upstream area remained selected across every regularized regression fold (Table S1.2). This convergence provides strong evidence for the role of porous geology, often contributing to high baseflow (and total discharge), as a mechanistically grounded control on thermal sensitivity, consistent with deep-infiltration and slow groundwater release through volcanic substrates (Tague et al. 2007).

The strong negative associations of High Cascades geology, BFI and total upstream area with thermal sensitivity are consistent with local and regional studies, including those examining extreme heat years (Chang and Psaris 2013; Isaak et al. 2016; Krochta and Chang 2024; Krochta et al. 2025; Mayer 2012; van Hamel and Brunner 2024). Hydrogeologic attributes were among the identified environmental controls on thermal sensitivity in Washington (McGill et al. 2024), while lower thermal sensitivity in boreal streams was associated with catchment morphology indicative of greater thermal buffering and inferred groundwater influence (Kamel et al. 2026). River temperature extremes in European mountain rivers were primarily driven by air temperature but strongly modified by baseflow conditions (van Hamel and Brunner 2024).

Land cover variability was also associated with spatial differences in thermal sensitivity. Lower percent upstream shrubland area in the MLR and SSN models (Tables 2 and 3) and high upstream vegetation height in the RF model (Figure 3) were all consistent with lower thermal sensitivity. This finding is consistent with Fuller et al. (2022), which found that riparian shade restoration could decrease stream temperature increases, particularly in smaller streams. Counterintuitively, upstream developed land area was negatively associated with thermal sensitivity in MLR Model 2 (Table 2). However, the RF ALE response indicated a nonlinear relationship, with thermal sensitivity increasing sharply across the lowest levels of developed land before gradually declining as developed land increased (Figure 3). Thus, the negative MLR coefficient was generally consistent with the declining RF response across most of the developed-land gradient (likely reflecting thermal inertia of larger streams), while the RF model additionally identified a nonlinear positive response that began at low levels of development (Timm et al. 2020; Wondzell et al. 2018). Percent upstream agricultural land cover's positive association with thermal sensitivity in the RF model may be attributed to activities such as irrigation and groundwater extraction, which can increase thermal sensitivity by reducing groundwater inputs and introducing warmer irrigation return flows (Ficklin et al. 2023; Ouellet et al. 2020).

While positive associations between shrubland area and thermal sensitivity are consistent with previous studies (Isaak et al. 2017;

10991085, 2026, 10, Downloaded from https://onlinelibrary.wiley.com/doi/10.1002/hyp.70745 by Portland State University, Wiley Online Library on [16/10/2026]. See the Terms and Conditions (https://onlinelibrary.wiley.com/terms-and-conditions) on Wiley Online Library for rules of use; OA articles are governed by the applicable Creative Commons License

Krochta et al. 2025), the negative coefficient for burned buffer area in the MLR Model 1 ($\beta = -0.25$; Table 2) was unexpected. Previous literature generally links wildfire burn area with increased stream temperature via riparian cover loss (Chen and Chang 2023; Koontz et al. 2018), the inverse relationship observed here may partly reflect the concentration of burned area in middle- and high-elevation catchments that are otherwise less thermally sensitive. Post-fire changes in snowmelt and recharge may also increase subsequent summer flows (Boisramé et al. 2019). In permeable catchments, reduced evapotranspiration and interception following fire may similarly increase recharge and baseflow, potentially buffering streams from air-temperature fluctuations (Bart and Tague 2017; Walvoord et al. 2025).

4.2 | Model Comparison

Although the three models consistently identified key predictors, the MLR and RF models do not account for spatial dependence associated with flow directionality and distance. The SSN models address this limitation by incorporating spatial covariance while retaining the same fixed-effect predictors as the MLRs (Table 3). Notably, while total upstream area and buffer burned area were significant predictors of stream thermal sensitivity in the non-spatial MLR models, they were not consistently significant in the SSN models, suggesting that their apparent effects may at least partly reflect spatial autocorrelation within the stream network (Table 3). The SSN model also had the largest LOOCV R^2 (0.85 for Model 2; Table 5), likely reflecting its explicit representation of residual spatial dependence through tail-up and Euclidean covariance structures (Ver Hoef and Peterson 2010). Previous studies similarly show that SSN models can explain more variation in stream temperatures than equivalent non-spatial MLR models (Mainali et al. 2019; O'Sullivan et al. 2020); Krochta and Chang (2024) found that an SSN model explained 94.4% of 7-day average maximum stream temperature variation compared with 81.2% for an aspatial MLR model within the Clackamas Basin.

While the SSN model had the greatest explanatory power with the lowest LOOCV RMSE (Table 3), the RF model's improvements of performance and error over MLR likely reflect RF's ability to account for non-linear relationships and interactions between variables (Corona and Hogue 2025; Wade et al. 2023). Its ensemble decision tree structure can capture interactions among diverse drivers that may be missed by traditional linear approaches (Feigl et al. 2021). Overall, the superior performances of the SSN and RF models indicate that accounting for spatial dependence and nonlinear relationships improves representation of the complex hydrogeologic and climatic controls on stream thermal sensitivity.

4.3 | Limitations and Implications for Future Directions and Climate Conditions

Although the 2021 Pacific Northwest heat dome represented an exceptionally warm summer within our observational record, recent work indicates that heatwaves are increasing disproportionately in duration, with the longest and most extreme events becoming increasingly likely as temperatures rise (Martinez-Villalobos et al. 2025). Though air temperature remains the dominant driver of stream temperature, hydrologic controls such as groundwater inputs become increasingly important during extreme thermal events (van Hamel and Brunner 2024; Sun et al. 2025). Despite sustained atmospheric and stream warming in 2021, thermal sensitivity increased modestly in the Clackamas River at Oregon City, Eagle Creek and Fish Creek, suggesting air–stream temperature coupling remained largely consistent during 2021 (Supporting Information Section S2).

Because thermal sensitivity was estimated only from July 1 to August 31, 2021, sampling additional sites and years would better characterize its controls and interannual variability. Additionally, the 4-km spatial resolution of PRISM may not fully capture fine-scale air temperature variability in the basin's complex terrain.

The relatively small sample size also limits the predictive application of the RF model to new or unobserved sites; here, RF was used primarily to identify potential nonlinear relationships and interactions not represented by the MLR. Future work could use hybrid geographically-weighted models (Mainali et al. 2023) and ML algorithms with more data to better resolve nonlinear and spatial relationships. Although the original analysis considered 40 landscape predictors, extensive collinearity among landscape and climatic predictors required a reduced variable selection and regularized regression process. These analyses increased confidence that High Cascades geology and BFI reflect genuine drivers of thermal sensitivity while indicating that several predictors retained in our original MLR model (including burned buffer area) were more fragile under resampling (Supporting Information Section S1).

Incorporating additional predictors including streamflow, snowpack and riparian canopy cover could more precisely identify factors regulating thermal sensitivity (McGill et al. 2024; Timm et al. 2021; Ulaski et al. 2023). Future work could also apply spatial and nonlinear models with projected climatic and landscape predictors to evaluate how thermal sensitivity and its controls may shift under future conditions (Hill et al. 2014; Isaak et al. 2017; Krochta et al. 2025; Winkowski 2023).

Understanding spatial variation in thermal sensitivity can inform management and conservation efforts aimed at protecting water resources and cold-water habitats (Krochta et al. 2025). Streams draining lowland areas may represent priorities for mitigating thermal impacts, while high-elevation streams underlain by porous geology provide valuable thermal refugia for salmonids.

5 | Conclusion

The drivers of stream thermal sensitivity are complex and significantly influenced by unique hydrogeologic, landscape and climatic factors inherently present across spatial gradients in a river basin. Our research suggests that in general, landscape predictors derived at the total upstream area scale were more consistently associated with thermal sensitivity when compared to landscape predictors derived at the reach contributing area scale and 100-m

10991085, 2026, 10, Downloaded from https://onlinelibrary.wiley.com/doi/10.1002/hyp.70745 by Portland State University, Wiley Online Library on [16/10/2026]. See the Terms and Conditions (https://onlinelibrary.wiley.com/terms-and-conditions) on Wiley Online Library for rules of use; OA articles are governed by the applicable Creative Commons License

wide buffer area scale. Specifically, although individual models differed in the predictors selected, MLR, SSN and RF models converged on a common set of underlying controls related to hydrogeology and land cover. High Cascades geology, BFI and upstream area repeatedly emerged as important predictors, collectively highlighting the influence of groundwater inputs and watershed hydrology on thermal sensitivity. Vegetation height, shrub cover, developed land and burned area were also identified across modelling approaches, indicating an additional role of land cover and disturbance processes. We illustrate these findings through deriving a MLR model from spatially derived landscape predictors and further validating thermal sensitivity drivers using SSN and RF models. Thus, variation in the specific predictors retained among models appears to reflect, at least in part, different indicators of shared underlying processes rather than fundamentally different explanations of stream thermal sensitivity.

Furthermore, this study distinguishes hydrologically robust drivers of stream thermal sensitivity from predictors susceptible to uncertainty associated with data-driven selection procedures (especially in small, spatially influenced watershed datasets prone to collinearity) through regularized regression techniques (ridge, LASSO and elastic net). However, we have suggested potential improvements including a more temporally and spatially comprehensive sampling, using predictors absent from this study (e.g., streamflow) and application of these models under projected future climatic and landscape conditions to better characterize controlling factors of thermal sensitivity.

Acknowledgements

This research was supported by the National Science Foundation under grant no. 2244551 through Portland State University's Research Experiences for Undergraduates (REU) program. We extend our gratitude to the anonymous reviewers whose thoughtful feedback significantly improved this manuscript. We also thank the agencies and contributors involved in the coordinated stream temperature data collection efforts that made this study possible. Figure 1 and the graphical abstract were created in *BioRender* (Milburn, S. (2026). *BioRender*. BioRender.com).

Funding

This work was supported by the National Science Foundation (2244551).

Conflicts of Interest

The authors declare no conflicts of interest.

Data Availability Statement

The data and code are available on GitHub (Milburn et al. 2026) at https://github.com/savpmilburn/What_Controls_Spatial_Variation_In_Thermal_Sensitivity_Cascades_River_Basin_During_Extreme_Heat_Year.

References

Altmann, A., L. Toloşi, O. Sander, and T. Lengauer. 2010. "Permutation Importance: A Corrected Feature Importance Measure." *Bioinformatics* 26, no. 10: 1340–1347. https://doi.org/10.1093/bioinformatics/btq134.

Apley, D. W., and J. Zhu. 2020. "Visualizing the Effects of Predictor Variables in Black Box Supervised Learning Models." *Journal of the Royal Statistical Society, Series B: Statistical Methodology* 82, no. 4: 1059–1086. https://doi.org/10.1111/rssb.12377.

Bart, R. R., and C. L. Tague. 2017. "The Impact of Wildfire on Baseflow Recession Rates in California." *Hydrological Processes* 31, no. 8: 1662–1673. https://doi.org/10.1002/hyp.11141.

Beaupré, L., A. St-Hilaire, A. Daigle, and N. Bergeron. 2020. "Comparison of a Deterministic and Statistical Approach for the Prediction of Thermal Indices in Regulated and Unregulated River Reaches: Case Study of the Fourchue River (Québec, Canada)." *Water Quality Research Journal* 55, no. 4: 394–408. https://doi.org/10.2166/wqrj.2020.001.

Benjamini, Y., and Y. Hochberg. 1995. "Controlling the False Discovery Rate: A Practical and Powerful Approach to Multiple Testing." *Journal of the Royal Statistical Society: Series B: Methodological* 57, no. 1: 289–300. https://doi.org/10.1111/j.2517-6161.1995.tb02031.x.

Boisramé, G., A. Harpold, and C. Tague. 2024. "Relationships Between Snowpack, Low Flows and Stream Temperature in Mountain Watersheds of the US West Coast." *Hydrological Processes* 38, no. 5: e15157. https://doi.org/10.1002/hyp.15157.

Boisramé, G., S. E. Thompson, C. Tague, and S. L. Stephens. 2019. "Restoring a Natural Fire Regime Alters the Water Balance of a Sierra Nevada Catchment." *Water Resources Research* 55, no. 7: 5751–5769. https://doi.org/10.1029/2018wr024098.

Bowerman, T., M. Keefer, and C. Caudill. 2021. "Elevated Stream Temperature, Origin, and Individual Size Influence Chinook Salmon Prespawn Mortality Across the Columbia River Basin." *Fisheries Research* 237: 105874. https://doi.org/10.1016/j.fishres.2021.105874.

Breiman, L. 2001. "Random Forests." *Machine Learning* 45, no. 1: 5–32. https://doi.org/10.1023/A:1010933404324.

Burnham, K. P., and D. R. Anderson. 2002. *Model Selection and Multimodel Inference: A Practical Information-Theoretic Approach*. Springer New York.

Caissie, D. 2006. "The Thermal Regime of Rivers: A Review." *Freshwater Biology* 51, no. 8: 1389–1406. https://doi.org/10.1111/j.1365-2427.2006.01597.x.

Chang, H., P. Loikith, and L. Messer. 2021. "The June 2021 Extreme Heat Event in Portland, OR, USA: Its Impacts on Ecosystems and Human Health and Potential Adaptation Strategies." *Journal of Extreme Events* 8, no. 3: 2175001. https://doi.org/10.1142/s2345737621750014.

Chang, H., and M. Psaris. 2013. "Local Landscape Predictors of Maximum Stream Temperature and Thermal Sensitivity in the Columbia River Basin, USA." *Science of the Total Environment* 461-462: 587–600. https://doi.org/10.1016/j.scitotenv.2013.05.033.

Chen, J., and H. Chang. 2023. "A Review of Wildfire Impacts on Stream Temperature and Turbidity Across Scales." *Progress in Physical Geography: Earth and Environment* 47, no. 3: 369–394. https://doi.org/10.1177/03091333221118363.

Clackamas County. 2022. *Streets Data Layer*. Clackamas County GIS Data Portal. https://www.clackamas.us/gis/data-portal.

Corona, C. R., and T. S. Hogue. 2025. "Machine Learning in Stream and River Water Temperature Modeling: A Review and Metrics for Evaluation." *Hydrology and Earth System Sciences* 29, no. 12: 2521–2549. https://doi.org/10.5194/hess-29-2521-2025.

Diaz, J., S. Oliver, and G. Gorski. 2025. "Evaluation of Daily Stream Temperature Predictions (1979-2021) Across the Contiguous United States Using a Spatiotemporal Aware Machine Learning Algorithm." *Environmental Modelling & Software* 193: 106655–106655. https://doi.org/10.1016/j.envsoft.2025.106655.

Drainas, K., L. Kaule, S. Mohr, B. Uniyal, R. Wild, and J. Geist. 2023. "Predicting Stream Water Temperature With Artificial Neural Networks Based on Open-Access Data." *Hydrological Processes* 37, no. 10: e14991. https://doi.org/10.1002/hyp.14991.

10991085, 2026, 10, Downloaded from https://onlinelibrary.wiley.com/doi/10.1002/hyp.70745 by Portland State University, Wiley Online Library on [16/10/2026]. See the Terms and Conditions (https://onlinelibrary.wiley.com/terms-and-conditions) on Wiley Online Library for rules of use; OA articles are governed by the applicable Creative Commons License

Dugdale, S., D. Hannah, and I. Malcolm. 2017. "River Temperature Modelling: A Review of Process-Based Approaches and Future Directions." *Earth-Science Reviews* 175: 97–113. https://doi.org/10.1016/j.earscirev.2017.10.009.

Dumelle, M., E. Peterson, J. Ver Hoef, A. Pearse, and D. Isaak. 2024. "SSN2: The Next Generation of Spatial Stream Network Modeling in R." *Journal of Open Source Software* 9, no. 99: 6389. https://doi.org/10.21105/joss.06389.

ESRI. 2022. *ArcGIS Pro (Version 3.0.0) [Computer Software]*. Environmental Systems Research Institute.

ESRI. 2026. *How Exploratory Regression works—ArcGIS Pro Documentation*. Environmental Systems Research Institute.

Feigl, M., K. Lebiedzinski, M. Herrnegger, and K. Schulz. 2021. "Machine-Learning Methods for Stream Water Temperature Prediction." *Hydrology and Earth System Sciences* 25, no. 5: 2951–2977. https://doi.org/10.5194/hess-25-2951-2021.

Ficklin, D. L., D. M. Hannah, N. Wanders, et al. 2023. "Rethinking River Water Temperature in a Changing, Human-Dominated World." *Nature Water* 1, no. 2: 125–128. https://doi.org/10.1038/s44221-023-00027-2.

Fryda, T., E. LeDell, N. Gill, et al. 2024. *h2o: R Interface for the 'H2O' Scalable Machine Learning Platform. R Package Version 3.44.0.3*. https://CRAN.R-project.org/package=h2o.

Fuller, M. R., P. Leinenbach, N. E. Detenbeck, R. Labiosa, and D. J. Isaak. 2022. "Riparian Vegetation Shade Restoration and Loss Effects on Recent and Future Stream Temperatures." *Restoration Ecology* 30, no. 7: e13626. https://doi.org/10.1111/rec.13626.

Hill, R. A., C. P. Hawkins, and J. Jin. 2014. "Predicting Thermal Vulnerability of Stream and River Ecosystems to Climate Change." *Climatic Change* 125, no. 3–4: 399–412. https://doi.org/10.1007/s10584-014-1174-4.

Hooker, G., L. Mentch, and S. Zhou. 2021. "Unrestricted Permutation Forces Extrapolation: Variable Importance Requires at Least One More Model, or There Is no Free Variable Importance." *Statistics and Computing* 31, no. 6: 82. https://doi.org/10.1007/s11222-021-10057-z.

Isaak, D. J., E. E. Peterson, J. M. Ver Hoef, et al. 2014. "Applications of Spatial Statistical Network Models to Stream Data." *Wiley Interdisciplinary Reviews: Water* 1, no. 3: 277–294. https://doi.org/10.1002/wat2.1023.

Isaak, D. J., S. J. Wenger, E. E. Peterson, et al. 2017. "The NorWeST Summer Stream Temperature Model and Scenarios for the Western U.S.: A Crowd-Sourced Database and New Geospatial Tools Foster a User Community and Predict Broad Climate Warming of Rivers and Streams." *Water Resources Research* 53, no. 11: 9181–9205. https://doi.org/10.1002/2017wr020969.

Isaak, D. J., M. K. Young, C. H. Luce, et al. 2016. "Slow Climate Velocities of Mountain Streams Portend Their Role as Refugia for Cold-Water Biodiversity." *Proceedings of the National Academy of Sciences* 113, no. 16: 4374–4379. https://doi.org/10.1073/pnas.1522429113.

Kamel, H., K. Prestegaard, and S. E. Ziegler. 2026. "Climate Sensitivity of Humid Boreal Forest Stream Water Sourcing Informed by Variation in Air-Stream Temperature Regression." *Hydrological Processes* 40, no. 7: e70607. https://doi.org/10.1002/hyp.70607.

Kaushal, S. S., G. E. Likens, N. A. Jaworski, et al. 2010. "Rising Stream and River Temperatures in the United States." *Frontiers in Ecology and the Environment* 8, no. 9: 461–466. https://doi.org/10.1890/090037.

Koontz, E. D., E. A. Steel, and J. D. Olden. 2018. "Stream Thermal Responses to Wildfire in the Pacific Northwest." *Freshwater Science* 37, no. 4: 731–746. https://doi.org/10.1086/700403.

Krochta, M., and K. Anlauf-Dunn. 2025. *Supporting Datasets for Article "Effects of Climate Change on Stream Temperature and Salmonid Habitats in a Cascades River Basin"*. HydroShare. https://doi.org/10.4211/hs.884d8badf48f4bc1a8dffc5c775de145.

Krochta, M., K. Anlauf-Dunn, D. Bugni, and H. Chang. 2025. "Effects of Climate Change on Stream Temperature and Salmonid Habitats in a Cascades River Basin." *Journal of Environmental Management* 387: 125843. https://doi.org/10.1016/j.jenvman.2025.125843.

Krochta, M., and H. Chang. 2024. "Scales of Connectivity Within Stream Temperature Networks of the Clackamas River Basin, Oregon." *Annals of the American Association of Geographers* 114, no. 8: 1653–1667. https://doi.org/10.1080/24694452.2023.2289981.

LANDFIRE. 2022. "Conterminous U.S. LANDFIRE - LF 2022 - Vegetation - Existing Vegetation Cover. U.S. Department of the Interior, Geological Survey, and U.S. Department of Agriculture." Accessed September 2026. http://www.landfire.gov/viewer.

Leach, J. A., C. Kelleher, B. L. Kurylyk, R. D. Moore, and B. T. Neilson. 2023. "A Primer on Stream Temperature Processes." *WIREs Water* 10, no. 4: e1643. https://doi.org/10.1002/wat2.1643.

Li, Z. 2024. "GeoShapley: A Game Theory Approach to Measuring Spatial Effects in Machine Learning Models." *Annals of the American Association of Geographers* 114, no. 7: 1365–1385. https://doi.org/10.1080/24694452.2024.2350982.

Luce, C., B. Staab, M. Kramer, S. Wenger, D. Isaak, and C. McConnell. 2014. "Sensitivity of Summer Stream Temperatures to Climate Variability in the Pacific Northwest." *Water Resources Research* 50, no. 4: 3428–3443. https://doi.org/10.1002/2013wr014329.

Mainali, J., H. Chang, and Y. Chun. 2019. "A Review of Spatial Statistical Approaches to Modeling Water Quality." *Progress in Physical Geography: Earth and Environment* 43, no. 6: 801–826. https://doi.org/10.1177/0309133319852003.

Mainali, J., H. Chang, and R. Parajuli. 2023. "Stream Distance-Based Geographically Weighted Regression for Exploring Watershed Characteristics and Water Quality Relationships." *Annals of the American Association of Geographers* 113, no. 2: 390–408. https://doi.org/10.1080/24694452.2022.2107478.

Martinez-Villalobos, C., D. Fu, P. C. Loikith, and J. D. Neelin. 2025. "Accelerating Increase in the Duration of Heatwaves Under Global Warming." *Nature Geoscience* 18, no. 8: 716–723. https://doi.org/10.1038/s41561-025-01737-w.

Mayer, T. D. 2012. "Controls of Summer Stream Temperature in the Pacific Northwest." *Journal of Hydrology* 475: 323–335. https://doi.org/10.1016/j.jhydrol.2012.10.012.

McGill, L. M., E. A. Steel, and A. H. Fullerton. 2024. "Empirical Stream Thermal Sensitivity Cluster on the Landscape According to Geology and Climate." *Hydrology and Earth System Sciences* 28, no. 6: 1351–1371. https://doi.org/10.5194/hess-28-1351-2024.

Molnar, C., G. Casalicchio, and B. Bischl. 2018. "Iml: An R Package for Interpretable Machine Learning." *Journal of Open Source Software* 3, no. 26: 786. https://doi.org/10.21105/joss.00786.

National Oceanic and Atmospheric Administration, Fisheries. 2021. *Run-timing Matters: Evolution, Plasticity, and Functional Extinction of Unique Pacific Salmon Populations. NOAA Fisheries*. https://www.fisheries.noaa.gov/west-coast/climate/run-timing-matters-evolution-plasticity-and-functional-extinction-unique-pacific.

Native Fish Society. 2022. *Clackamas River*. NFS. https://nativefishsociety.org/learn/watersheds/clackamas-river.

Nolin, A. W. 2012. "Perspectives on Climate Change, Mountain Hydrology, and Water Resources in the Oregon Cascades, USA." *Mountain Research and Development* 32, no. S1: S35–S46. https://doi.org/10.1659/MRD-JOURNAL-D-11-00038.S1.

Oregon Department of Geology and Mineral Industries (DOGAMI). 2020. *Geologic Map of Oregon*. DOGAMI. https://gis.dogami.oregon.gov/maps/geologicmap/.

10991085, 2026, 10, Downloaded from https://onlinelibrary.wiley.com/doi/10.1002/hyp.70745 by Portland State University, Wiley Online Library on [16/10/2026]. See the Terms and Conditions (https://onlinelibrary.wiley.com/terms-and-conditions) on Wiley Online Library for rules of use; OA articles are governed by the applicable Creative Commons License

O'Sullivan, A. M., K. J. Devito, J. Ogilvie, et al. 2020. "Effects of Topographic Resolution and Geologic Setting on Spatial Statistical River Temperature Models." *Water Resources Research* 56, no. 12: e2020WR028122. https://doi.org/10.1029/2020wr028122.

Ouellet, V., A. St-Hilaire, S. J. Dugdale, D. M. Hannah, S. Krause, and S. Proulx-Ouellet. 2020. "River Temperature Research and Practice: Recent Challenges and Emerging Opportunities for Managing Thermal Habitat Conditions in Stream Ecosystems." *Science of the Total Environment* 736: 139679. https://doi.org/10.1016/j.scitotenv.2020.139679.

Peterson, E. E., and J. M. Ver Hoef. 2010. "A Mixed-Model Moving-Average Approach to Geostatistical Modeling in Stream Networks." *Ecology* 91, no. 3: 644–651. https://doi.org/10.1890/08-1668.1.

PRISM. 2021. *PRISM Group*. Oregon State University. https://prism.oregonstate.edu.

R Core Team. 2024. *R: A Language and Environment for Statistical Computing. R Foundation for Statistical Computing*. https://www.R-project.org/.

Roberts, D. R., V. Bahn, S. Ciuti, et al. 2017. "Cross-Validation Strategies for Data With Temporal, Spatial, Hierarchical, or Phylogenetic Structure." *Ecography* 40, no. 8: 913–929. https://doi.org/10.1111/ecog.02881.

Siegel, J. E., A. H. Fullerton, A. M. FitzGerald, D. Holzer, and C. E. Jordan. 2023. "Daily Stream Temperature Predictions for Free-Flowing Streams in the Pacific Northwest, USA." *PLOS Water* 2, no. 8: e0000119. https://doi.org/10.1371/journal.pwat.0000119.

Siegel, J. E., and C. J. Volk. 2019. "Accurate Spatiotemporal Predictions of Daily Stream Temperature From Statistical Models Accounting for Interactions Between Climate and Landscape." *PeerJ* 7: e7892. https://doi.org/10.7717/peerj.7892.

Starcevich, S. J. 2021. *Clackamas River Bull Trout Reintroduction Project: Characterizing Status, Trend, and Thermal Habitat Suitability in 2020*. Oregon Department of Fish and Wildlife, Native Fish Investigations Program. https://odfwnfi.forestry.oregonstate.edu/reports.

State of Oregon Department of Environmental Quality. 2019. *Updated Source Water Assessment, Clackamas River Public Water Systems*. Oregon DEQ. https://www.deq.state.or.us/wq/dwp/docs/uswareports/USWA_00187.00580.00591Clackamas.pdf.

State of Oregon Department of Environmental Quality. 2025. *TMDLs for the Willamette Subbasins*. Oregon DEQ. https://www.oregon.gov/deq/wq/tmdls/pages/tmdlrwillamette.aspx.

Sun, J., R. Graf, D. Wrzesiński, et al. 2025. "Impact of Extreme Atmospheric Heat Events on River Thermal Dynamics and Heatwaves." *Journal of Hydrology* 659: 133292. https://doi.org/10.1016/j.jhydrol.2025.133292.

Tague, C., M. Farrell, G. Grant, S. Lewis, and S. Rey. 2007. "Hydrogeologic Controls on Summer Stream Temperatures in the McKenzie River Basin, Oregon." *Hydrological Processes* 21, no. 24: 3288–3300. https://doi.org/10.1002/hyp.6538.

Tague, C., G. Grant, M. Farrell, J. Choate, and A. Jefferson. 2008. "Deep Groundwater Mediates Streamflow Response to Climate Warming in the Oregon Cascades." *Climatic Change* 86, no. 1: 189–210. https://doi.org/10.1007/s10584-007-9294-8.

Tibshirani, R. 1996. "Regression Shrinkage and Selection via the Lasso." *Journal of the Royal Statistical Society, Series B: Statistical Methodology* 58, no. 1: 267–288. https://doi.org/10.1111/j.2517-6161.1996.tb02080.x.

Timm, A., V. Ouellet, and M. Daniels. 2020. "Swimming Through the Urban Heat Island: Can Thermal Mitigation Practices Reduce the Stress?" *River Research and Applications* 36, no. 10: 1973–1984. https://doi.org/10.1002/rra.3732.

Timm, A., V. Ouellet, and M. Daniels. 2021. "Riparian Land Cover, Water Temperature Variability, and Thermal Stress for Aquatic Species in Urban Streams." *Water* 13, no. 19: 2732. https://doi.org/10.3390/w13192732.

Tredennick, A. T., G. Hooker, S. P. Ellner, and P. B. Adler. 2021. "A Practical Guide to Selecting Models for Exploration, Inference, and Prediction in Ecology." *Ecology* 102, no. 6: e03336. https://doi.org/10.1002/ecy.3336.

Ulaski, M. E., L. Warkentin, S. M. Naman, and J. W. Moore. 2023. "Spatially Variable Effects of Streamflow on Water Temperature and Thermal Sensitivity Within a Salmon-Bearing Watershed in Interior British Columbia, Canada." *River Research and Applications* 39, no. 10: 2036–2047. https://doi.org/10.1002/rra.4200.

U.S. Geological Survey (USGS), U.S. Forest Service (USFS), and K. Nelson. 2022. *Monitoring Trends in Burn Severity*. U.S. Geological Survey data release. https://doi.org/10.5066/P9IED7RZ.

U.S. Geological Survey, National Hydrography Dataset Plus (USGS). 2012. NHDPlus Version 2. https://nhdplus.com/NHDPlus/.

USGS. 2021. "Annual National Land Cover Database." Assessed on September 2026. https://www.usgs.gov/centers/eros/science/annual-national-land-cover-database.

van Hamel, A., and M. I. Brunner. 2024. "Trends and Drivers of Water Temperature Extremes in Mountain Rivers." *Water Resources Research* 60, no. 10: e2024WR037518. https://doi.org/10.1029/2024WR037518.

Ver Hoef, J. M., E. Peterson, and D. Theobald. 2006. "Spatial Statistical Models That Use Flow and Stream Distance." *Environmental and Ecological Statistics* 13, no. 4: 449–464. https://doi.org/10.1007/s10651-006-0022-8.

Ver Hoef, J. M., and E. E. Peterson. 2010. "A Moving Average Approach for Spatial Statistical Models of Stream Networks." *Journal of the American Statistical Association* 105, no. 489: 6–18. https://doi.org/10.1198/jasa.2009.ap08248.

Ver Hoef, J. M., E. E. Peterson, D. Clifford, and R. Shah. 2014. "SSN: An R Package for Spatial Statistical Modeling on Stream Networks." *Journal of Statistical Software* 56, no. 3: 1–45. https://doi.org/10.18637/jss.v056.i03.

Wade, J., C. Kelleher, and D. M. Hannah. 2023. "Machine Learning Unravels Controls on River Water Temperature Regime Dynamics." *Journal of Hydrology* 623: 129821–129821. https://doi.org/10.1016/j.jhydrol.2023.129821.

Walvoord, M. A., B. A. Ebel, T. F. Partridge, D. M. Rey, and D. O. Rosenberry. 2025. "Disparate Groundwater Responses to Wildfire." *Wiley Interdisciplinary Reviews Water* 12, no. 3: e70029. https://doi.org/10.1002/wat2.70029.

Wehrly, K. E., T. O. Brenden, and L. Wang. 2009. "A Comparison of Statistical Approaches for Predicting Stream Temperatures Across Heterogeneous Landscapes." *JAWRA Journal of the American Water Resources Association* 45, no. 4: 986–997. https://doi.org/10.1111/j.1752-1688.2009.00341.x.

Weierbach, H., A. R. Lima, J. Willard. et al., 2022. "Stream Temperature Predictions for River Basin Management in the Pacific Northwest and Mid-Atlantic Regions Using Machine Learning." *Water* 14, no. 7: 1032–1032. https://doi.org/10.3390/w14071032.

Winkowski, J. J. 2023. *Updating Spatial Stream Network Models of August Stream Temperature for the Washington Coast Salmon Recovery Region*. *Washington Department of Fish and Wildlife*. FPT 23-04. https://wdfw.wa.gov/publications/02445.

Wondzell, S. M., M. Diabat, and R. Haggerty. 2018. "What Matters Most: Are Future Stream Temperatures More Sensitive to Changing Air Temperatures, Discharge, or Riparian Vegetation?" *JAWRA Journal of the American Water Resources Association* 55, no. 1: 116–132. https://doi.org/10.1111/1752-1688.12707.

10991085, 2026, 10, Downloaded from https://onlinelibrary.wiley.com/doi/10.1002/hyp.70745 by Portland State University, Wiley Online Library on [16/10/2026]. See the Terms and Conditions (https://onlinelibrary.wiley.com/terms-and-conditions) on Wiley Online Library for rules of use; OA articles are governed by the applicable Creative Commons License

Wright, M. N., and A. Ziegler. 2017. "Ranger: A Fast Implementation of Random Forests for High Dimensional Data in C++ and R." *Journal of Statistical Software* 77, no. 1: 1–17. https://doi.org/10.18637/jss.v077.i01.

Zou, H., and T. Hastie. 2005. "Regularization and Variable Selection via the Elastic Net." *Journal of the Royal Statistical Society, Series B: Statistical Methodology* 67, no. 2: 301–320. https://doi.org/10.1111/j.1467-9868.2005.00503.x.

Supporting Information

Additional supporting information can be found online in the Supporting Information section. **Supporting Information: S1.** Supporting Information Section S1. Regularized Regression Results. **Table S1:1** Pooled R^2 values across methods, lambda selection criteria and an unregularized ordinary least squares diagnostic. All methods were run under a geographic five-fold cross-validation. **Table S1:2** Percentage of folds out of five in which each predictor's coefficient was retained (non-zero) in the full candidate pool under ridge, LASSO and elastic net regularized regression. Note: ridge regression never sets a coefficient to zero; thus, its column is 100% by construction. **Supporting Information: Section S2 Table S2:** Bootstrap comparison of stream thermal sensitivity during the 2021 Pacific Northwest heat dome and all other sampled years at three long-term monitoring sites. Values represent the difference in thermal sensitivity (TS Difference; 2021 minus the mean of all other years), with accompanying 95% percentile bootstrap confidence intervals. Positive values indicate higher thermal sensitivity during 2021 relative to the historical mean **Figure S2:1** Summer 2021 air and stream temperatures compared with conditions during all other sampled years. Stream temperatures are shown for Eagle Creek, Fish Creek and Oregon City sample locations and mean air temperature represents the daily average across the three sites. Dark blue lines show daily temperatures during 2021, while light blue lines show the mean daily temperature across all non-2021 years. Shaded ribbons indicate the daily minimum-to-maximum range observed among non-2021 years. The comparison highlights the anomalously high atmospheric and stream temperatures associated with the June 2021 Pacific Northwest heat dome and the persistence of elevated stream temperatures later in the summer. **Figure S2:2** Comparison of stream thermal sensitivity during the 2021 Pacific Northwest heat dome and all other sampled years at three long-term monitoring sites. Blue circles represent the 2021 thermal sensitivity estimate, while boxplots and grey points summarize the distribution of estimates from all other years.

10991085, 2026, 10, Downloaded from https://onlinelibrary.wiley.com/doi/10.1002/hyp.70745 by Portland State University, Wiley Online Library on [16/10/2026]. See the Terms and Conditions (https://onlinelibrary.wiley.com/terms-and-conditions) on Wiley Online Library for rules of use; OA articles are governed by the applicable Creative Commons License